Jaroslav Pospíšil

The experimental comparison of statistical methods for measurement of the optical transfer function of objectives

Acta Universitatis Palackianae Olomucensis. Facultas Rerum Naturalium. Mathematica-Physica-Chemica, Vol. 11 (1971), No. 1, 233--248

Persistent URL: http://dml.cz/dmlcz/119942

1971 — ACTA UNIVERSITATIS PALACKIANAE OLOMUCENSIS
FACULTAS RERUM NATURALIUM — TOM 33

Katedra experimentální fyziky a metodiky fyziky
Vedoucí katedry: Prof. Paed. dr. Josef Fuka

THE EXPERIMENTAL COMPARISON OF STATISTICAL METHODS FOR MEASUREMENT OF THE OPTICAL TRANSFER FUNCTION OF OBJECTIVES

JAROSLAV POSPÍŠIL

(Received March 10th, 1970)

1. INTRODUCTION

This article describes the experiment for comparison of statistical cross-correlation and statistical auto-correlation methods for obtaining the optical transfer function of objectives in the case of incoherent image formation. Some results related to the photographic objective are introduced and both mentioned methods are evaluated.

2. THEORETICAL CONSIDERATIONS

The theory of statistical cross-correlation method and statistical auto-correlation method and the description of their realizations are introduced in papers [1] and [2]. Following article [1], we can express the optical transfer function as follows:

$$g(\sigma, \vartheta) = \frac{\varphi_{oi}(\sigma, \vartheta)_n}{\varphi_{oo}(\sigma, \vartheta)_n}, \tag{1}$$

where

$$\varphi_{oi}(\sigma, \vartheta)_n = \frac{\varphi_{oi}(\sigma, \vartheta)}{\varphi_{oi}(0, 0)}, \tag{2}$$

$$\varphi_{oo}(\sigma, \vartheta)_n = \frac{\varphi_{oo}(\sigma, \vartheta)}{\varphi_{oo}(0, 0)}, \tag{3}$$

$$\varphi_{oi}(\sigma, \vartheta) = \int_{-\infty}^{\infty}\int \Phi_{oi}(\varepsilon, \eta)_0 \exp\left[-i\,2\pi(\sigma\varepsilon + \vartheta\eta)\right] \mathrm{d}\varepsilon\,\mathrm{d}\eta, \tag{4}$$

$$\varphi_{oi}(0, 0) = \int_{-\infty}^{\infty}\int \Phi_{oi}(\varepsilon, \eta)_0 \,\mathrm{d}\varepsilon\,\mathrm{d}\eta, \tag{5}$$

$$\varphi_{oo}(\sigma, \vartheta) = \int_{-\infty}^{\infty}\int \Phi_{oo}(\varepsilon, \eta)_0 \exp\left[-i\,2\pi(\sigma\varepsilon + \vartheta\eta)\right] \mathrm{d}\varepsilon\,\mathrm{d}\eta, \tag{6}$$

$$\varphi_{oo}(0, 0) = \iint_{-\infty}^{\infty} \Phi_{oo}(\varepsilon, \eta)_0 \, d\varepsilon \, d\eta. \tag{7}$$

$\Phi_{oi}(\varepsilon, \eta)_0$ is the cross-correlation function of the averaged stationary random signal (object) and its image produced by linear and isoplanatic optical system; ε and η denote the shifts in rectangular directions. $\Phi_{oo}(\varepsilon, \eta)_0$ is the averaged auto-correlation function of the stationary random chart. $\varphi_{oi}(\sigma, \vartheta)_n$ and $\varphi_{oo}(\sigma, \vartheta)_n$ are the normalized Fourier transformations of functions $\Phi_{oi}(\varepsilon, \eta)_0$ and $\Phi_{oo}(\varepsilon, \eta)_0$, so called the normalized cross-spectrum and the normalized object power spectrum, σ and ϑ are the spatial frequencies expressed in lines per millimeter (L/mm) in the directions ε and η expressed in millimeters. If

$$\varepsilon \to \infty, \qquad \eta \to \infty, \tag{8}$$

then

$$\Phi_{oi}(\varepsilon, \eta)_0 = 0, \tag{9}$$

$$\Phi_{oo}(\varepsilon, \eta)_0 = 0. \tag{10}$$

By means of equations (2) as far (7), the equation (1) becomes as follows:

$$g(\sigma, \vartheta) = \frac{\iint_{-\infty}^{\infty} \Phi_{oo}(\varepsilon, \eta)_0 \, d\varepsilon \, d\eta \iint_{-\infty}^{\infty} \Phi_{oi}(\varepsilon, \eta)_0 \exp\left[-i\,2\pi(\sigma\varepsilon + \vartheta\eta)\right] d\varepsilon \, d\eta}{\iint_{-\infty}^{\infty} \Phi_{oi}(\varepsilon, \eta)_0 \, d\varepsilon \, d\eta \iint_{-\infty}^{\infty} \Phi_{oo}(\varepsilon, \eta)_0 \exp\left[-i\,2\pi(\sigma\varepsilon + \vartheta\eta)\right] d\varepsilon \, d\eta}. \tag{11}$$

We can to write the one-dimensional analogy of equation (11) in the form

$$g(\sigma) = \frac{\int_{-\infty}^{\infty} \Phi_{oo}(\varepsilon)_0 \, d\varepsilon \int_{-\infty}^{\infty} \Phi_{oi}(\varepsilon)_0 \exp\left(-i\,2\pi\sigma\varepsilon\right) d\varepsilon}{\int_{-\infty}^{\infty} \Phi_{oi}(\varepsilon)_0 \, d\varepsilon \int_{-\infty}^{\infty} \Phi_{oo}(\varepsilon)_0 \exp\left(-i\,2\pi\sigma\varepsilon\right) d\varepsilon}. \tag{13}$$

By means of Euler equation

$$\exp\left(-i\,2\pi\sigma\varepsilon\right) = \cos 2\pi\sigma\varepsilon - i \sin 2\pi\sigma\varepsilon, \tag{14}$$

we can express the equation (13) as follows:

$$g(\sigma) = q \, \frac{\int_{-\infty}^{\infty} \Phi_{oi}(\varepsilon)_0 \cos 2\pi\sigma\varepsilon \, d\varepsilon - i \int_{-\infty}^{\infty} \Phi_{oi}(\varepsilon)_0 \sin 2\pi\sigma\varepsilon \, d\varepsilon}{\int_{-\infty}^{\infty} \Phi_{oo}(\varepsilon)_0 \cos 2\pi\sigma\varepsilon \, d\varepsilon - i \int_{-\infty}^{\infty} \Phi_{oo}(\varepsilon)_0 \sin 2\pi\sigma\varepsilon \, d\varepsilon}, \tag{15}$$

where

$$q = \frac{\int_{-\infty}^{\infty} \Phi_{oo}(\varepsilon)_0 \, d\varepsilon}{\int_{-\infty}^{\infty} \Phi_{oi}(\varepsilon)_0 \, d\varepsilon}. \tag{16}$$

In the case of on- axis image conditions is

$$\int_{-\infty}^{\infty} \Phi_{oi}(\varepsilon)_0 \sin 2\pi\sigma\varepsilon \, d\varepsilon = 0, \tag{17}$$

$$\int_{-\infty}^{\infty} \Phi_{oo}(\varepsilon)_0 \sin 2\pi\sigma\varepsilon \, d\varepsilon = 0, \tag{18}$$

then

$$g(\sigma) = \tau(\sigma) \exp[-i\Theta(\sigma)] = \tau(\sigma). \tag{19}$$

From equation (19) follows, that the phase transfer function $\Theta(\sigma)$ is in the case of on-axis image conditions zero (except of the case of spurious resolution in which is $\Theta(\sigma) = (2k - 1)\pi$, $k = 1, 2, 3, \ldots$). The function $\tau(\sigma)$ is called the modulation transfer function.

From equations (13), (17) and (18) follows:

$$\tau(\sigma) = q \frac{\int_{-\infty}^{\infty} \Phi_{oi}(\varepsilon)_0 \cos 2\pi\sigma\varepsilon \, d\varepsilon}{\int_{-\infty}^{\infty} \Phi_{oo}(\varepsilon)_0 \cos 2\pi\sigma\varepsilon \, d\varepsilon}. \tag{20}$$

The equation (20) is fundamental for the measurements by means of the statistical cross-correlation method in realization according to Fig. 1 and Fig. 3.

From article [2] follows, that the statistical auto-correlation method is based on the following expression:

$$\tau(\sigma, \vartheta) = \left[\frac{\varphi_{ii}(\sigma, \vartheta)_n}{\varphi_{oo}(\sigma, \vartheta)_n}\right]^{\frac{1}{2}}, \tag{21}$$

where

$$\varphi_{oo}(\sigma, \vartheta)_n = \frac{\varphi_{oo}(\sigma, \vartheta)}{\varphi_{oo}(0, 0)}, \tag{22}$$

$$\varphi_{ii}(\sigma, \vartheta)_n = \frac{\varphi_{ii}(\sigma, \vartheta)}{\varphi_{ii}(0, 0)}, \tag{23}$$

$$\varphi_{oo}(\sigma, \vartheta) = 2 \int_0^{\infty}\int \Phi_{oo}(\varepsilon, \eta)_0 \cos 2\pi(\sigma\varepsilon + \vartheta\eta) \, d\varepsilon \, d\eta, \tag{24}$$

$$\varphi_{oo}(0, 0) = 2 \int_0^{\infty}\int \Phi_{oo}(\varepsilon, \eta)_0 \, d\varepsilon \, d\eta, \tag{25}$$

$$\varphi_{ii}(\sigma, \vartheta) = 2 \int_0^{\infty}\int \varphi_{ii}(\varepsilon, \eta)_0 \cos 2\pi(\sigma\varepsilon + \vartheta\eta) \, d\varepsilon \, d\eta, \tag{26}$$

$$\varphi_{ii}(0, 0) = 2 \int_0^{\infty}\int \Phi_{ii}(\varepsilon, \eta)_0 \, d\varepsilon \, d\eta. \tag{27}$$

$\Phi_{ii}(\varepsilon, \eta)_0$ is the symmetric auto-correlation function of the averaged stationary random image produced by imaging of a stationary random chart by linear and isoplanatic optical system. $\varphi_{ii}(\sigma, \vartheta)_n$ is the normalized Fourier transformation of

function $\Phi_{ii}(\varepsilon, \eta)_0$, so called the normalized image power spectrum. In the case of conditions (8) is:

$$\Phi_{ii}(\varepsilon, \eta)_0 = 0. \tag{28}$$

Substituting from (22) far as (27) into (21), we obtain:

$$\tau(\sigma, \vartheta) = \left[\frac{\int_0^\infty \int \Phi_{oo}(\varepsilon, \eta)_0 \, d\varepsilon \, d\eta \quad \int_0^\infty \int \Phi_{ii}(\varepsilon, \eta)_0 \cos 2\pi(\sigma\varepsilon + \vartheta\eta) \, d\varepsilon \, d\eta}{\int_0^\infty \int \Phi_{ii}(\varepsilon, \eta)_0 \, d\varepsilon \, d\eta \quad \int_0^\infty \int \Phi_{oo}(\varepsilon, \eta)_0 \cos 2\pi(\sigma\varepsilon + \vartheta\eta) \, d\varepsilon \, d\eta} \right]^{\frac{1}{2}}. \tag{29}$$

In the one-dimensional case the equation (29) becomes as follows:

$$\tau(\sigma) = \left[r \frac{\int_0^\infty \Phi_{ii}(\varepsilon)_0 \cos 2\pi\sigma\varepsilon \, d\varepsilon}{\int_0^\infty \Phi_{oo}(\varepsilon)_0 \cos 2\pi\sigma\varepsilon \, d\varepsilon} \right]^{\frac{1}{2}}, \tag{30}$$

where

$$r = \frac{\int_0^\infty \Phi_{oo}(\varepsilon)_0 \, d\varepsilon}{\int_0^\infty \Phi_{ii}(\varepsilon)_0 \, d\varepsilon}. \tag{31}$$

From equations (21) and (30) follows, that by the statistical auto-correlation method we receive only the modulation transfer function $\tau(\sigma)$. The equation (30) is fundamental for the measurements by the statistical auto-correlation method in realization according to Fig. 1 and Fig. 3.

3. THE MEASURING PROCEDURE AND THE DESCRIPTION OF THE MEASURING EQUIPMENT

By both mentioned statistical methods were measured the on-axis modulation transfer functions $\tau(\sigma)$ of photographic objectives under the same image conditions for mutual comparison. Fig. 1 shows the measuring procedure. *IE* denotes the imaging equipment shown in Fig. 2 and Fig. 3. The imaging process is produced by the photographic objective under test *TL* on a fine-grain photographic emulsion *E*. The image on the processed photographic emulsion *E* was evaluated by the optical correlator *OC*. The two-samples optical correlator was used. Its construction is in accordance with schema in Fig. 4 ([3], [4]).

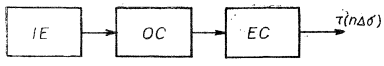

Fig. 1. The schema of measuring procedure by statistical cross-correlation and statistical auto-correlation methods.

By mutual parallel shift ε of two samples SA_1 and SA_2 with constant velocity, we obtain their correlation function. If the samples are the same random charts (or the same images of random chart produced by objective under test on a suitable photographic emulsion E after its developing), we obtain the auto-correlation function $\Phi_{oo}(\varepsilon)$ ($\Phi_{ii}(\varepsilon)$). If one sample is the random chart and the second one is its image of the same size on a suitable photographic emulsion E after its developing, we obtain the cross-correlation function $\Phi_{oi}(\varepsilon)$.

From the obtained functions $\Phi_{oo}(\varepsilon)$, $\Phi_{ii}(\varepsilon)$ and $\Phi_{oi}(\varepsilon)$ were determined the functions $\Phi_{oo}(\varepsilon)_0$, $\Phi_{ii}(\varepsilon)_0$ and $\Phi_{oi}(\varepsilon)_0$. By means of equations (20) and (30) in the forms:

$$\tau(n\,\Delta\sigma) = q\,\frac{\sum_{k=0}^{m}\Phi_{oi}(k\,\Delta\varepsilon)_0\cos(2\pi n\,\Delta\sigma k\,\Delta\varepsilon)\,\Delta\varepsilon}{\sum_{k=0}^{m}\Phi_{oo}(k\,\Delta\varepsilon)_0\cos(2\pi n\,\Delta\sigma k\,\Delta\varepsilon)\,\Delta\varepsilon}, \tag{32}$$

$$\tau(n\,\Delta\sigma) = \left[r\,\frac{\sum_{k=0}^{m}\Phi_{ii}(k\,\Delta\varepsilon)_0\cos(2\pi n\,\Delta\sigma k\,\Delta\varepsilon)\,\Delta\varepsilon}{\sum_{k=0}^{m}\Phi_{oo}(k\,\Delta\varepsilon)_0\cos(2\pi n\,\Delta\sigma k\,\Delta\varepsilon)\,\Delta\varepsilon}\right]^{\frac{1}{2}}, \tag{33}$$

where

$$q = \frac{\sum_{k=0}^{m}\Phi_{oo}(k\,\Delta\varepsilon)_0\,\Delta\varepsilon}{\sum_{k=0}^{m}\Phi_{oi}(k\,\Delta\varepsilon)_0\,\Delta\varepsilon},$$

$$r = \frac{\sum_{k=0}^{m}\Phi_{oo}(k\,\Delta\varepsilon)_0\,\Delta\varepsilon}{\sum_{k=0}^{m}\Phi_{ii}(k\,\Delta\varepsilon)_0\,\Delta\varepsilon},$$

were obtained values $\tau(n\,\Delta\sigma)$ of the modulation transfer function $\tau(\sigma)$ of the photographic objective under test. The calculations of equations (32) and (33) were made by electronic computer EC (*TOSBAC 3121*, Toshiba Electric Co., Japan). The used sampling values $\Delta\varepsilon$, $\Delta\sigma$ and m correspond with the sampling theorem [5] ($k = 0, 1, 2, \ldots, m$; $n = 0, 1, 2, \ldots$).

The random chart was made by photographic way in accordance with papers [1], [6] and [7]. By uniform illumination of the fine-grain photographic emulsion Fuji Plate – Process Panchromatic, *12 ASA*, after processing and enlargement of processed mentioned photographic emulsion with magnification about 300 on the emulsion Fuji Plate Hard, *1 ASA*, was obtained practically a stationary random chart (see photograph in Fig. 5). Fig. 6 shows the auto-correlation function of the realized random chart. Its normalized power spectrum is in Fig. 7.

For obtaining uniform illumination of the random chart *RCH* in the imaging equipment *IE*, was used the flat light source *S* (Photoreflector Lamp Toshiba, Flood

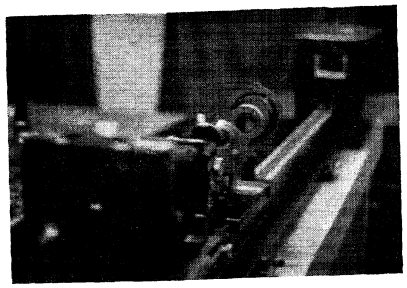

Fig. 2. The photograph of imaging equipment.

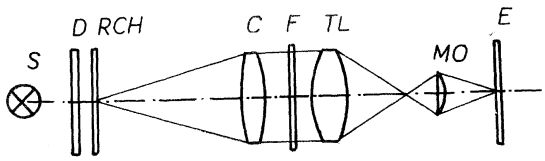

Fig. 3. The optical system of the imaging equipment.

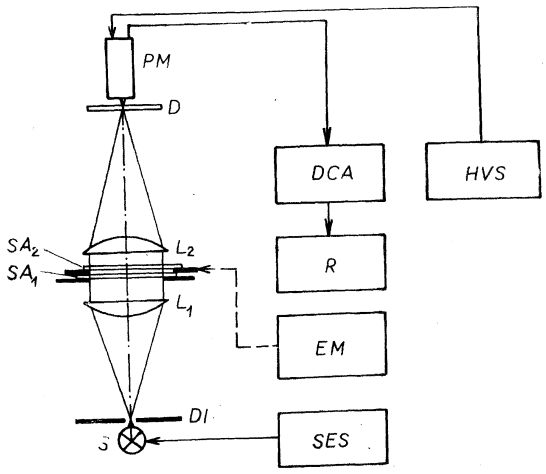

Fig. 4. The schema of two-samples optical correlator.

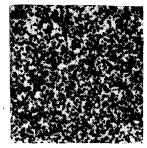

Fig. 5. The photograph of used random chart.

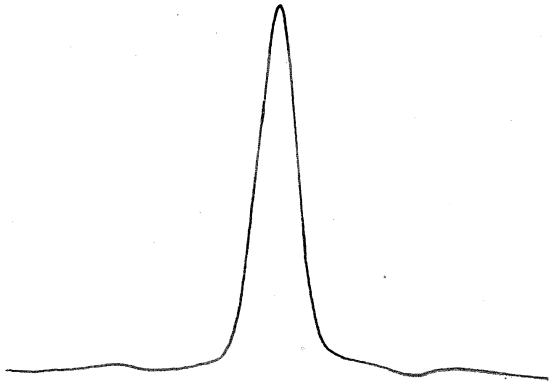

Fig. 6. The record of random chart auto-correlation function.

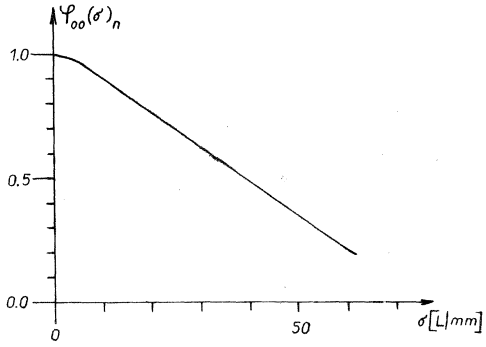

Fig. 7. The normalized power spectrum of the used random chart.

100 *V*, 500 *W*) and a diffusing plate *D*. *C* in Fig. 3 is the collimating objective (Nippon Kogaku, $f = 1\,191.1$ mm) for obtaining the parallel light beams entranced to the photographic objective under test *TL*. *MO* is a suitable planachromatic microscope objective with large numerical aperture for enlargement of the image by objective under test *TL*. The final image on the photographic emulsion *E* has the same size as the random chart RCH (the over-all magnification is unity). The colour filter F enables measurements in colour light.

The used illuminating range covered only the linear part of the photographic emulsion — modified characteristic curve in the form $T = T(E)$, where T is the transmittance and E is the effective exposure. Then the nonlinear influence of the used photographic emulsion was negligible. The linear distortion of the used microscope objective *MO* and of the used photographic emulsion *E* was also negligible, because of the large magnification of the microscope objective. Also, the influence of the collimating objective *C* was practically negligible.

The used two-samples correlator (Fig. 4) consists of the light source *S* (Lamp Olympus Tokyo, 6 *V*, 5 *A*), diaphragm *DI*, two lenses L_1 and L_2, diffusion plate *D*, photomultiplier *PM* (Photomultiplier *PM* — 49 Hamamatsu), direct current amplifier *DCA* and pen recorder *R* (Hitachi Perkin-Elmer Recorder 159). *HVS* is the high voltage source (Precission Power Source, Model *VS* — 100 *BR*) for the photomultiplier *PM*. *SES* is the stabilized direct current source (Electronic Measurements Eatontown, N. I., Programable Regatron) for supplying the light source *S*. The travel of the light beam from source *S* is shown from Fig. 3. During action of the described optical correlator the samples SA_1 and SA_2 move in oposite directions by influence of the electric motor *EM*. The used anode voltage of the photomultiplier (500 *V*) and the used range of illumination, entranced to the photomultiplier, caused negligible influence of linear and nonlinear distortions of the correlator eqiupment.

4. RESULTS

Three examples of measurement of the modulation transfer functions $\tau(\sigma)_{cr}$ and $\tau(\sigma)_a$ by statistical cross-correlation and statistical auto-correlation methods are introduced in this section. The results relate to the on-axis image condition and colour light ($\lambda = 5\,875$ Å). The objective under test was photographic objective Auto-Takumar Asahi Opt. Co., $1 : 3.5$, $f = 35$ mm. The photographic emulsion used for indication of random chart images was Fuji Plate Process Panchromatic, *12 ASA*. Processing was made by Fuji Microfine developer and Fuji Fujifix fixing agent in accordance with the factory instructions.

The first example is related to the best visual focus position ($\Delta z = 0.0$ mm) for the relative aperture $1 : 3.5$ of the objective under test and the second example is related to the best visual focus position ($\Delta z = 0.0$ mm) and for the relative aperture $1 : 16$ of the objective under test. The results of the third example are for relative

aperture 1 : 3.5 of the objective under test and for the defocusing $\Delta z = -0.09$ mm. The results are expressed in the form of tables and graphs. The used differences

$$\Delta(\sigma)_{cra} = \tau(\sigma)_{cr} - \tau(\sigma)_a,$$

show the degree of agreement of results by both statistical methods.

The accuracy of results $\tau(\sigma)_{cr}$ and $\tau(\sigma)_a$ is expressed by absolute errors

$$\Delta(\sigma)_{cr} = \tau(\sigma)_{cr} - \tau(\sigma)_c,$$
$$\Delta(\sigma)_a = \tau(\sigma)_a - \tau(\sigma)_c,$$

where functions $\tau(\sigma)_c$ are the expected results.

4.1. RESULTS FOR $\Delta z = 0.0$ mm AND RELATIVE APERTURE 1 : 3.5

Table 1: Results related to the part 4.1.

σ [L/mm]	$\varphi_{oo}(\sigma)_n$	$\varphi_{oi}(\sigma)_n$	$\varphi_{ii}(\sigma)_n$	$\tau(\sigma)_{cr}$	$\tau(\sigma)_a$	$\tau(\sigma)_c$	$\Delta(\sigma)_{cr}$	$\Delta(\sigma)_a$	$\Delta(\sigma)_{cra}$
0.0	1.000	1.000	1.000	1.000	1.000	1.000	0.000	0.000	0.000
3.4	0.983	0.990	0.984	1.007	1.000	0.987	0.020	0.013	—0.007
6.8	0.940	0.963	0.938	1.023	0.999	0.956	0.067	0.043	—0.024
10.2	0.884	0.919	0.871	1.040	0.993	0.950	0.090	0.043	—0.047
13.6	0.831	0.861	0.795	1.036	0.978	0.937	0.099	0.041	—0.058
17.0	0.790	0.793	0.724	1.008	0.957	0.912	0.096	0.045	—0.049
20.4	0.757	0.719	0.550	0.950	0.863	0.862	0.088	0.001	—0.087
23.8	0.718	0.640	0.525	0.894	0.875	0.850	0.044	0.025	—0.019
27.2	0.664	0.562	0.472	0.846	0.843	0.812	0.034	0.031	—0.003
30.6	0.592	0.488	0.399	0.824	0.821	0.800	0.024	0.021	—0.003
34.0	0.516	0.419	0.335	0.812	0.806	0.794	0.018	0.012	—0.006
37.4	0.452	0.355	0.281	0.785	0.788	0.775	0.010	0.013	0.003
40.8	0.408	0.299	0.238	0.733	0.764	0.750	—0.017	0.014	0.031
44.2	0.383	0.250	0.200	0.653	0.723	0.737	—0.084	—0.014	0.070
47.6	0.358	0.207	0.166	0.578	0.681	0.700	—0.122	—0.019	0.103
51.0	0.322	0.170	0.137	0.528	0.652	0.681	—0.153	—0.029	0.124
54.4	0.272	0.138	0.114	0.507	0.647	0.650	—0.143	—0.003	0.140
57.8	0.220	0.111	0.093	0.504	0.650	0.625	—0.121	0.025	0.146
61.2	0.179	0.088	0.078	0.492	0.660	0.600	—0.108	0.060	0.168

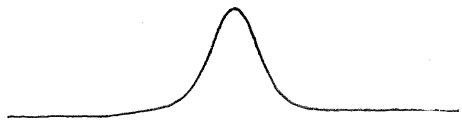

Fig. 8. The record of cross-correlation function related to imaging conditions described in part 4.1. of this article.

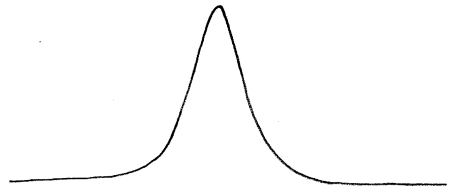

Fig. 9. The record of auto-correlation function related to imaging conditions described in part 4.1. of this article.

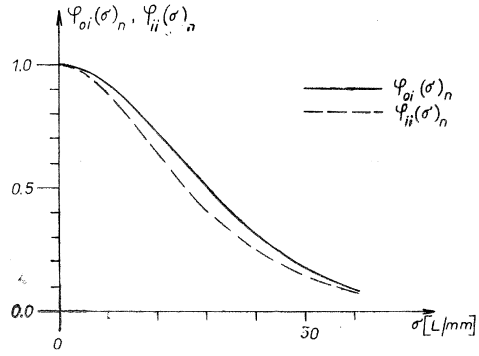

Fig. 10. The normalized power spectrums related to imaging conditions described in part 4.1. of this article.

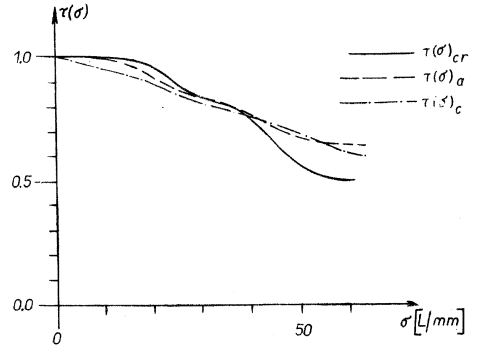

Fig. 11. The modulation transfer functions related to imaging conditions described in the part 4.1. of this article.

4.2. RESULTS FOR $\Delta z = 0.0$ mm AND RELATIVE APERTURE 1 : 16

Table 2: Results related to the part 4.2.

σ [L/mm]	$\varphi_{oo}(\sigma)_n$	$\varphi_{oi}(\sigma)_n$	$\varphi_{ii}(\sigma)_n$	$\tau(\sigma)_{cr}$	$\tau(\sigma)_a$	$\tau(\sigma)_c$	$\Delta(\sigma)_{cr}$	$\Delta(\sigma)_a$	$\Delta(\sigma)_{cra}$
0.0	1.000	1.000	1.000	1.000	1.000	1.000	0.000	0.000	0.000
3.4	0.983	0.976	0.967	0.993	0.992	0.975	0.018	0.017	0.001
6.8	0.940	0.909	0.876	0.967	0.965	0.962	0.005	0.003	0.002
10.2	0.884	0.817	0.720	0.924	0.902	0.900	0.024	0.002	0.042
13.6	0.831	0.714	0.581	0.859	0.836	0.850	0.009	—0.014	0.023
17.0	0.790	0.617	0.481	0.781	0.780	0.800	—0.019	—0.020	0.001
20.4	0.757	0.534	0.350	0.705	0.679	0.762	—0.057	—0.083	0.026
23.8	0.718	0.466	0.307	0.649	0.654	0.750	—0.101	—0.096	—0.005
27.2	0.664	0.407	0.263	0.613	0.629	0.687	—0.074	—0.058	—0.016
30.6	0.592	0.354	0.233	0.598	0.627	0.650	—0.052	—0.023	—0.029
34.0	0.516	0.303	0.207	0.578	0.633	0.625	—0.038	—0.008	—0.146
37.4	0.452	0.254	0.178	0.562	0.627	0.600	—0.038	0.027	—0.065
40.8	0.408	0.207	0.145	0.507	0.596	0.537	—0.030	0.059	—0.089
44.2	0.383	0.165	0.112	0.431	0.541	0.525	—0.094	0.016	—0.110
47.6	0.358	0.131	0.081	0.366	0.476	0.500	—0.134	—0.024	—0.110
51.0	0.322	0.104	0.057	0.323	0.421	0.475	—0.152	—0.054	—0.098
54.4	0.272	0.084	0.039	0.309	0.379	0.400	—0.091	—0.021	—0.070
57.8	0.220	0.071	0.029	0.323	0.363	0.375	—0.052	—0.012	—0.040

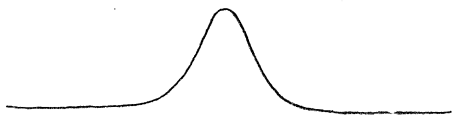

Fig. 12. The record of cross-correlation function related to imaging conditions described in part 4.2. of this article.

Fig. 13. The record of auto-correlation function related to imaging conditions described in part 4.2. of this article.

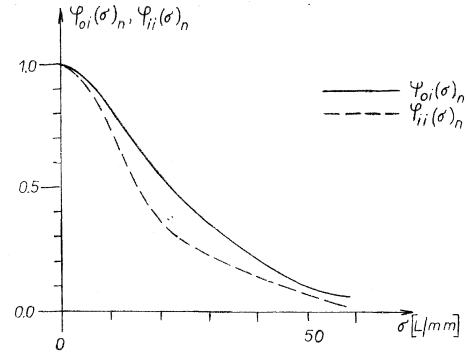

Fig. 14. The normalized power spectrums related toimaging conditions described in part 4.2. of this article.

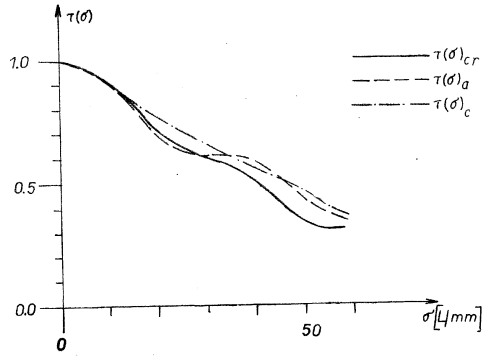

Fig. 15. The modulation transfer functions related to imaging conditions described in part 4.2. of this article.

4.3. RESULTS FOR $\Delta z = -0.09$ mm AND RELATIVE APERTURE 1:3.5

Table 3: Results related to the part 4.3.

σ [L/mm]	$\varphi_{oo}(\sigma)_n$	$\varphi_{oi}(\sigma)_n$	$\varphi_{ii}(\sigma)_n$	$\tau(\sigma)_{cr}$	$\tau(\sigma)_a$	$\tau(\sigma)_c$	$\Delta(\sigma)_{cr}$	$\Delta(\sigma)_a$	$\Delta(\sigma)_{cra}$
0.0	1.000	1.000	1.000	1.000	1.000	1.000	0.000	0.000	0.000
3.4	0.983	0.968	0.943	0.985	0.979	0.975	0.010	0.004	—0.006
6.8	0.940	0.882	0.812	0.938	0.929	0.931	0.007	—0.002	—0.009
10.2	0.884	0.784	0.673	0.889	0.872	0.900	—0.011	—0.028	—0.017
13.6	0.831	0.670	0.614	0.806	0.859	0.862	—0.056	—0.003	0.053
17.0	0.790	0.632	0.591	0.800	0.865	0.825	—0.025	0.040	0.065
20.4	0.757	0.562	0.555	0.742	0.856	0.775	—0.033	0.081	0.114
23.8	0.718	0.468	0.464	0.652	0.804	0.712	—0.060	0.092	0.152
27.2	0.664	0.351	0.327	0.529	0.702	0.537	—0.008	0.165	0.173
30.6	0.592	0.233	0.194	0.393	0.572	0.500	—0.107	0.072	0.179
34.0	0.516	0.138	0.109	0.267	0.460	0.437	—0.170	0.023	0.193
37.4	0.452	0.079	0.074	0.175	0.405	0.387	—0.212	0.018	0.230

Fig. 16. The record of cross-correlation function related to imaging conditions described in part 4.3. of this article.

Fig. 17. The record of auto-correlation function related to imaging conditions described in part 4.3. of this article.

5. CONCLUSIONS

The obtained results show approximate agreement of functions $\tau(\sigma)_{cr}$, $\tau(\sigma)_a$ and $\tau(\sigma)_c$ in the frequency ranges shown in Fig. 11, 15 and 19. The errors $\Delta(\sigma)_a$ are mostly smaller than differences $\Delta(\sigma)_{cr}$ and $\Delta(\sigma)_{cra}$. The analysis of many results obtained for various image conditions shows, that both statistical methods in the described realization give reproductionaly results for on-axis image condition, white and monochromatic light, for the best visual focus image position and for small amounts of

defocusing of the image. The described realization is mostly suitable for measurements by statistical auto-correlation method, but results obtained by statistical cross-correlation method are also practically sufficient for middle and mostly for low spatial frequencies.

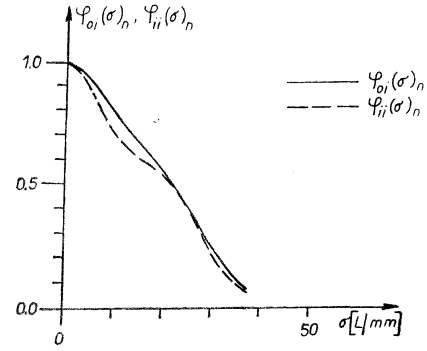

Fig. 18. The normalized power spectrums related to imaging conditions described in part 4.3. of this article.

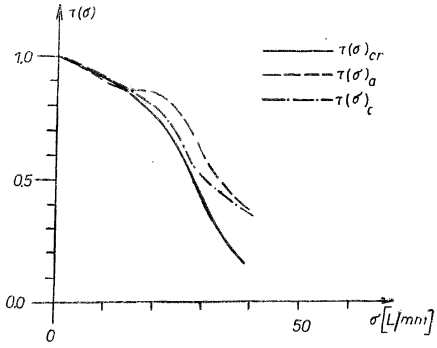

Fig. 19. The modulation transfer function related to imaging conditions described in part 4.3. of this article.

The both analyzed statistical methods in the described realization have the following main advantages: a high light efficiency, simple equipment and measurement, the possibility of measurement also in the case of magnification of the objective under test different from unity (this is the main difference and advantage in comparison with the equipment described in article [1]).

Main disadvantages are as follows: slow measurement, it is possible obtain only the modulation transfer function (not the phase transfer function), the error influence of the realized random chart.

Both tested statistical methods have only laboratory use in the present time.

REFERENCES

[1] *Kubota H., Ohzu H.:* J. Opt. Soc. Am., **47** (1957), 666.
[2] *Pospíšil J.:* Optik, **29** (1969), 379.
[3] *Kretzmer E. R.:* The Bell Syst. Tech. J., **31** (1952), 75.
[4] *Ooue Sh., Hatanaka I.:* Scientific Publ. Fuji Photo Film Co., LTD., **24** (1961), 24.
[5] *O'Neill E. L.:* Introduction to Statistical Optics, Addison-Wesley Publ. Co., INC., Reading Massachusetts—Polo Alto—London (1963), 163.
[6] *Tamura M., Kubota H.:* Oyo Butsuri, **26** (1957), 92.
[7] *Ohzu H., Kubota H.:* Oyo Butsuri, **26** (1957), 96.

Shrnutí

EXPERIMENTÁLNÍ SROVNÁNÍ STATISTICKÝCH METOD PRO MĚŘENÍ OPTICKÉ PŘENOSOVÉ FUNKCE OBJEKTIVŮ

JAROSLAV POSPÍŠIL

V článku je popsán experiment pro srovnání statistické metody vzájemné korelace a statistické metody autokorelace pro zjišťování optické přenosové funkce objektivů v případě nekoherentního zobrazení. Jsou ukázány některé výsledky měření optické přenosové funkce fotografického objektivu oběma zmíněnými metodami a obě metody jsou zhodnoceny.

Резюме

ЭКСПЕРИМЕНТАЛЬНОЕ СРАВНЕНИЕ СТАТИЧЕСКИХ МЕТОДОВ ДЛЯ ИЗМЕРЕНИЯ ФУНКЦИИ КОНТРАСТНОСТИ ОБЪЕКТИВОВ

ЯРОСЛАВ ПОСПИШИЛ

В статье описан эксперимент для сравнения статического метода взаимной корреляции и статического метода автокорреляции для установления функции контрастности объективов в случае некогерентного изображения. Дальше, в статье показаны некоторые результаты измерения функции контрастности фотографического объектива обоими упомянутыми методами и сделана оценка обоих методов.